Available online at www.sciencedirect.com
ScienceDirect
Applied Catalysis B: Environmental 80 (2008) 88–97
APPLIED CATALYSIS B: ENVIRONMENTAL
www.elsevier.com/locate/apcatb

Modification of the photocatalytic activity of Pd/TiO_2 and Zn/TiO_2 systems through different oxidative and reductive calcination treatments

M.A. Aramendía [a], V. Borau [a], J.C. Colmenares [a], A. Marinas [a,*], J.M. Marinas [a], J.A. Navío [b], F.J. Urbano [a]

[a] *Organic Chemistry Department, University of Córdoba, Campus de Rabanales, Marie Curie Building E-14014, Córdoba, Spain*
[b] *Instituto de Ciencia de Materiales de Sevilla, Centro Mixto Universidad de Sevilla-CSIC, Américo Vespucio s/n, E-41092, Sevilla, Spain*

Received 6 August 2007; received in revised form 2 November 2007; accepted 11 November 2007
Available online 24 November 2007

Abstract

Two different solids consisting of Pd or Zn-containing titania systems (metal/titanium nominal ratio of 1%) were submitted to diverse oxidative and reductive calcination treatments and tested for gas-phase selective photooxidation of 2-propanol. As regards the Pd system, reduction at low temperature (≤500 °C) resulted in a gradual increase in catalytic activity which was ascribed to the gradual reduction of bulk palladium to Pd^0. Thermal treatment of the system at high temperature (850 °C) in static air, air flow or hydrogen flow led to a decrease in activity as the result of the sharp decrease in surface area. Nevertheless, those systems containing Pd^0 only were more active than the one consisting of Pd + PdO. Finally, Pd-system overcame Pd migration to the surface on reduction at 850 °C which resulted in a significant increase in selectivity to acetone up to 97% for a time on stream of 5 h. As regards the Zn-containing system, none of the applied treatments resulted in improvement in photocatalytic activity. It seems that the most favourable situation for photocatalysis is that on which Zn atoms are substituting titanium ones in the lattice, whereas segregation of Zn to form small ZnO clusters is especially detrimental to activity.
© 2007 Elsevier B.V. All rights reserved.

Keywords: Photocatalysis; Selective photooxidation; Titania-based catalysts; Paladium-doped catalyst; Zinc-doped catalyst; 2-Propanol; Strong metal-support interaction (SMSI) effect

1. Introduction

Titania is a material widely used in photocatalysis though it presents two main drawbacks: (i) the low use of solar spectrum and (ii) its relatively high electron–hole recombination rate. One of the methods essayed to overcome such problems is doping with metals [1,2]. Moreover, photocatalytic properties of titania are influenced by some other features such as surface area, crystal phases present or precursor used.

As regards evaluation of photocatalytic properties of materials, different model molecules are generally tested, such as phenol [3], methylene blue [4] or stearic acid [5]. In the case of working in non-aqueous media, degradation of the tested chemical can be controlled, thus avoiding complete mineralization. In this sense, gas-phase selective photooxidation of 2-propanol to acetone is a relatively easy test reaction [6–8].

In a previous paper [9], several titania systems were synthesized by the sol–gel method using two different titanium precursors (titanium isopropoxide or tetrachloride) and diverse ageing methods (magnetic stirring, sonication, reflux and microwave radiation). Screening of such different synthetic conditions led us to choose titanium isopropoxide as the titanium precursor and sonication as the method of choice for ageing the gel, since such conditions ensured obtaining systems with relatively high surface area and consisting of 100% anatase particles which resulted in a better catalytic performance in gas-phase selective photooxidation of 2-propanol. Application of the method to the synthesis of a platinum-doped system resulted in a solid with a BET surface area of 57 m^2/g and consisted of 100% anatase titania. The system was submitted to different oxidative and reductive calcinations treatments in order to study the effect of such treatments on

* Corresponding author. Tel.: +34 957218622; fax: +34 957212066.
E-mail address: alberto.marinas@uco.es (A. Marinas).

0926-3373/$ – see front matter © 2007 Elsevier B.V. All rights reserved.
doi:10.1016/j.apcatb.2007.11.017

catalytic performance in the above-mentioned 2-propanol test reaction. Interestingly, oxidation or reduction of the systems at 850 °C (a value much higher than calcination temperature of the gel −500 °C) resulted in an increase in catalytic activity and selectivity to acetone. XPS analyses of the systems showed that thermal treatments at 850 °C resulted in electron transfer from titania to Pt^0 particles through the so-called strong metal–support interaction (SMSI) effect [10–12]. Furthermore, the greater the SMSI effect, the better the catalytic performance. Improvement in photocatalytic activity was explained in terms of avoidance of electron–hole recombination through the electron transfer from titania to platinum particles.

These interesting results prompted us to expand the study to the effect of such oxidation/reduction calcination treatments on the catalytic performance of two other systems obtained under identical conditions as the Pt/TiO_2 system but changing the dopant to Pd and Zn, respectively [6]. The former, as a group VIII element, could be expected to behave in a similar way as Pt-system thus exhibiting the SMSI effect. As for the latter, it has been widely used as dopant and ZnO itself exhibits photocatalytic activity, the possible synergetic Ti-Zn effect consequently being worth studying.

2. Experimental

2.1. Synthesis of different titania-based systems

The synthesis of the untreated palladium or zinc-containing titania systems was described in a previous paper [6]. To summarize, it was carried out through the sol–gel process, using titanium isopropoxide and Zn(II) or Pd(II) acetylacetonates as the Ti, Zn and Pd precursor, respectively, and NH_4OH (pH 9) as the precipitation agent. Gels were aged under ultrasonic irradiation for 10 h, subsequently dried at 110 °C for 24 h, ground and shifted to fine power (particle diameter below 0.149 mm). Finally, xerogels were calcined at 500 °C for 6 h in static air, thus obtaining the systems labelled as Pd-AS or Zn-AS, the suffix AS standing for ''as synthesized'' in order to differentiate them from subsequent thermal treatments.

Calcination of Pd-AS in a H_2/Ar (10:90 v/v) flow at 200 °C, 350 °C, 500 °C or 850 °C for 1 h yielded the systems labelled as Pd-200-H, Pd-350-H, Pd-500-H and Pd-850-H, respectively. On the other hand, oxidation of Pd-AS either in synthetic air flow or in a furnace in static air at 850 °C for 1 h led to the systems labelled as Pd-850-AIR and Pd-850-F, respectively.

Similarly, calcination of Zn-AS at 850 °C in a H_2/Ar flow, synthetic air flow or in a furnace in static air led to the systems labelled as Zn-850-H, Zn-850-AIR and Zn-850-F, respectively.

Finally, for comparative purposes the corresponding pure titania system (TiO_2-AS) was synthesized under identical conditions as described for Pd-AS and Zn-AS systems. Subsequent thermal treatment of TiO_2-AS at 850 °C under static air, hydrogen or synthetic air flow yielded the systems labelled as TiO_2-850-F, TiO_2-850-H or TiO_2-850-AIR, respectively.

2.2. Characterization

Elemental analysis of Pd and Zn-containing samples was carried out by the staff at the Central Service for the support of research (SCAI) at the University of Córdoba by inductively coupled plasma-mass spectrometry (ICP-MS). Measurement was made on a ICP-MS ELAN-DRC-e (Perkin-Elmer), after dissolution of the sample in a H_2SO_4:HF:H_2O (1:1:1) mixture. Atomic spectroscopy standards PE Pure Plus (Perkin-Elmer) were used for calibration.

Transmission electron microscopy (TEM) images (carried out at the SCAI of the University of Córdoba) were recorded in a JEOL JEM 2010 microscope operating at an accelerating voltage of 200 kV. The structural resolution of this microscope is 0.19 nm. Samples were mounted on 3-mm holey carbon copper grids. Moreover, the microscope was equipped with an energy dispersive X-ray analyses (EDX) detector.

The textural properties of solids (specific surface area, pore volume and mean pore radius) were determined from nitrogen adsorption–desorption isotherms at liquid nitrogen temperature by using a Micromeritics ASAP-2010 instrument. Surface areas were calculated by the Brunnauer-Emmett-Teller (BET) method, while pore distributions were determined by the Barrett-Joiner-Halenda (BJH) method. Prior to measurements, all samples were degassed at 110 °C to 0.1 Pa.

X-ray analysis of solids was carried out using a Siemens D-5000 diffractometer provided with an automatic control and data acquisition system (DACO-MP). The patterns were run with nickel-filtered copper radiation (λ = 1.5406 Å) at 40 kV and 30 mA; the diffraction angle 2θ was scanned at a rate of 2°/min. The average crystallite size of anatase and rutile was determined according to the Scherrer equation using the full-width at half-maximum (FWHM) of the peak corresponding to 101 and 110 reflections, respectively, and taking into account the instrument broadening.

Temperature-programmed reduction (TPR) analyses were performed on a Micromeritics TPD-TPR 2900 analyzer. 200 mg of catalysts were placed in the sample holder and reduced in a 45 mL/min H_2/Ar (10:90) flow. Temperature was ramped between 0 and 850 °C at 10 °C/min. The final temperature was kept for 1 h and the catalyst was then cooled down to room temperature in an Ar flow (45 mL/min). In the case of Pd-system, once TPR profile had been registered, new reductive treatments were carried out on the fresh sample at intermediate temperatures (200 °C, 350 °C and 500 °C) and 850 °C, which yielded the systems Pd-200-H, Pd-350-H, Pd-500-H and Pd-850-H, respectively. As for Zn-system, reduction at 850 °C led to the system labelled as Zn-850-H.

X-ray photoelectron spectroscopy (XPS) data were recorded on 4 mm × 4 mm pellets, 0.5 mm thick, prepared by slightly pressing the powdered materials which were outgassed in the prechamber of the instrument at 150 °C up to a pressure $\leq 2 \times 10^{-8}$ Torr to remove chemisorbed volatile species (water, CO, etc.) from their surfaces. The Leibold-Heraeus LHS10 spectrometer main chamber, working at a pressure $\leq 2 \times 10^{-9}$ Torr, was equipped with an EA-200 MCD hemispherical electron analyzer with a dual X-ray source working with Al Kα

($h\upsilon$ = 1486.6 eV) at 120 W, 30 mA using C(1s) as energy reference (284.6 eV).

2.3. Photocatalytic reaction

In photocatalytic experiments, 20 mL/min of a He:O_2 (90:10 v/v) mixture previously bubbled through 2-propanol at 0 °C was allowed into the photocatalytic reactor (2-propanol gas flow was measured to be ca. 8 μmol/min), in which 30 mg of powder catalyst had been placed. UV light (UV Spotlight source Lightningcure™ L8022, Hamamatsu, maximum emission at 365 nm) was focalized on the sample compartment (8 mm in diameter × 3 mm deep) through an optic fiber. Radiant flux in the catalyst compartment was measured to be 1.1 W/cm^2 (Hamamatsu UV-meter, C6080-03 Model). Reactor was on-line connected to a HP6890 chromatograph equipped with a six-way valve, a HP-PLOTU column (30 m long, 0.53 mm ID, 20 μm film thickness) and a Ni methanator (Agilent Part Number G2747A) which allowed us to determine the percentage of CO_2 resulting from mineralization of 2-propanol. Further details on the photocatalytic device are given elsewhere [6].

3. Results and discussion

3.1. Case study #1: Pd containing system

Some of the main features concerning characterization of Pd-AS system (reported in a previous paper [6]) are summarized in Table 1. As can be seen, it consists of 100% anatase titania particles, with a crystallite size of ca. 18 nm and a BET surface area of 75 m^2/g. Experimental Pd/Ti ratio (as determined by ICP-MS) is slightly higher than the nominal one (0.6 and 1%, respectively). Moreover, a comparison of ICP-MS and XPS results (indicative of bulk and surface composition, respectively) seems to suggest that palladium is preferentially placed on the surface, though no evidence for palladium crystal phases is seen by XRD (Fig. 1A), thus suggesting small crystallite size.

Pd-AS was tested for gas-phase selective photoxidation of 2-propanol (Fig. 2) exhibiting lower activities and selectivities to acetone than the corresponding bare-titania (TiO_2-AS). Therefore, for instance, initial 2-propanol conversion is 31.6 and 38.6% for Pd-AS and TiO_2-AS, respectively. The difference in activity increases with time-on-stream since Pd-AS exhibits a higher deactivation, which is not compensated by higher selectivity to acetone (e.g. conversions of 24.5 and 38.2% and selectivity of 73% and 76% at t = 5 h, for Pd-AS and TiO_2-AS, respectively).

In an attempt at improving photocatalytic performance of Pd-AS and gaining more information on the role of the metal, such system was submitted to different oxidation and reduction calcination treatments. Initially, a TPR profile of the solid was registered. As can be seen in Fig. 3, it showed four main reduction peaks centered at 88, 273, 400 and 599 °C. Palladium is known to be an easily reduced species even at subambient temperatures [13,14] although peaks at temperatures as high as ca. 300 °C have been attributed to the reduction of PdO particles that strongly interact with the support [15]. On the other hand, according to Ozkan et al. [14] the peaks observed at T ≤ 400 °C could be due to the reaction of H_2 with surface oxygen. In any case, the valleys between the observed peaks at ca. 200, 350 and 500 °C seem to be appropriate reduction temperatures as to reflect structural/compositional differences among the samples. Therefore, new systems were obtained on reduction of Pd-AS at 200, 350, 500 and 850 °C. For comparative purposes, the corresponding solids resulting from oxidation of Pd-AS at 850 °C in static air (Pd-850-F) or in synthetic air flow (Pd-850-AIR) were also synthesized. Some data concerning characterization of the solids are summarized in Table 1. As can be seen, the reduction of Pd-AS at temperatures below 500 °C (temperature at which its precursor gel was calcined) hardly leads to any change in textural or structural properties of the systems. Therefore, the resulting solids consist of anatase particles with crystallite size between 18 and 20 nm and a BET surface area of ca. 70 m^2/g. On the other hand, reduction at 500 °C results in a slight decrease in

Table 1
Summary of the most remarkable features concerning characterization of Pd- and Zn-containing titania systems

Photocatalyst	XRD		N_2 isotherms	ICP-MS	XPS
	Crystal phases[a] (%)	Crystallite size (nm)	S_{BET} (m^2/g)	Metal/Ti atomic%	Metal/Ti atomic%[b]
Pd-850-F	72%R, 28%A + PdO	72 (R), 61 (A)	8	ND[c]	0.5
Pd-850-AIR	93%R, 7%A + PdO + Pd	116 (R), 66 (A)	7	ND	0.8
Pd-AS	100%A	18	75	0.6	0.9
Pd-200-H	100%A	18	73	ND	0.9
Pd-350-H	100%A	20	75	ND	ND
Pd-500-H	100%A	21	62	ND	0.8
Pd-850-H	100%R	81	5	ND	3.1
Zn-850-F	100%R	81	6	ND	ND
Zn-850-AIR	100%R	66	5	0.7	14.3
Zn-AS	100%A	19	59	0.7	3.3
Zn-850-H	100%R	61	3	0.3	–[d]

[a] A and R denote anatase and rutile, respectively.
[b] Quantification of Pd/Ti and Zn/Ti atomic% present at the surface of systems was carried out though integration of Pd3d, Ti2p and Zn2p peaks.
[c] ND stands for "not determined".
[d] Quantification of zinc atomic% present at the surface of Zn-850-H was not possible since the intensity of Zn (2p) peak was very small.

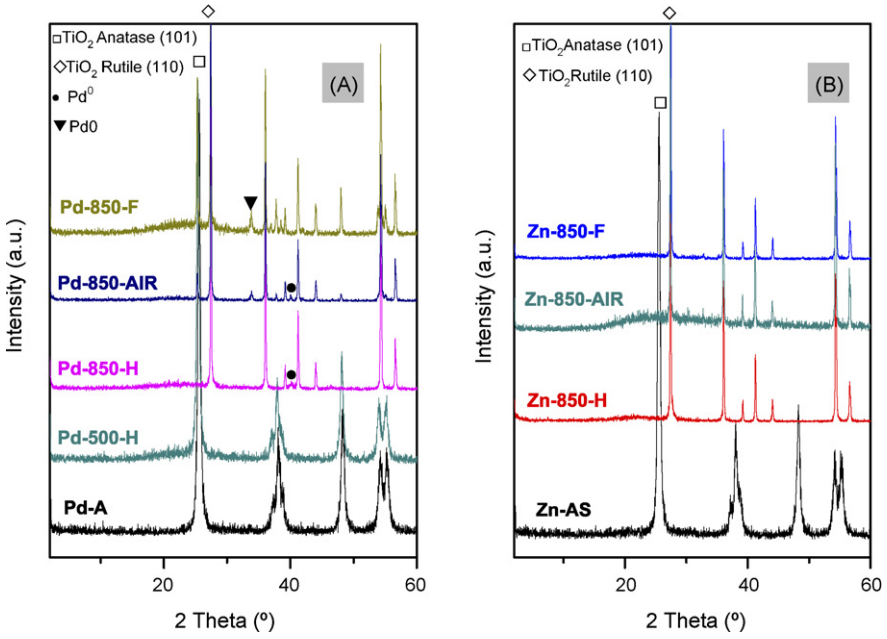

Fig. 1. X-ray diffraction patterns corresponding to the Pd (A) and Zn (B) contaning titania.

surface area while any treatment at 850 °C leads to a sharp drop in BET area, the systems changing from 100% anatase particles to mainly-rutile ones. Interestingly, reduction at 850 °C leads to 100% rutile whereas some anatase is present in systems calcined in air flow (7%) and especially in static air (28%). XRD pattern of some of the systems are shown in Fig. 1A. The ones corresponding to Pd-200-H and Pd-350-H (not represented) are similar to that of Pd-500-H. From Fig. 1A it is clear that thermal treatments at 850 °C lead to the appearance of palladium crystal phases which is indicative of an increase in particle size. As expected, the system reduced at 850 °C (Pd-850-H) exhibit Pd^0 particles at ca. $2\theta = 40.0$ (1 1 1 reflection) [16–18]. More interestingly, calcination either in static air or synthetic air flow leads to different palladium species. Therefore, in the former case both Pd (1 1 1 reflection at $2\theta = 40.0°$) and PdO (1 0 1 reflection at $2\theta = 33.9°$) [19,20] can be seen, whereas only PdO is observed in the latter. The formation of Pd^0 under oxidant conditions can be ascribed to

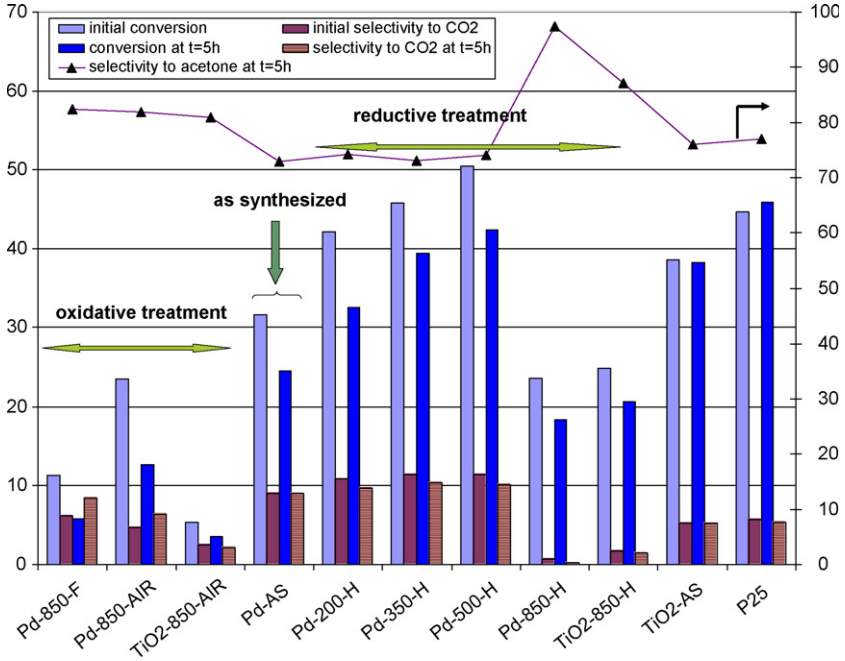

Fig. 2. Results obtained for gas-phase selective photooxidation of 2-propanol with all the Pd-containing titania described in the present study in terms of molar conversion (%), selectivity to acetone (%) and selectivity to CO_2 (%). For the sake of comparison, results obtained with the corresponding bare-titania systems as well as Degussa P25 have also been included.

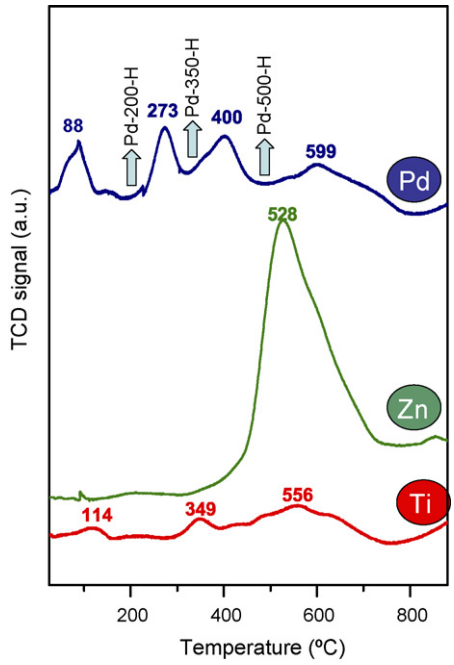

Fig. 3. TPR profiles of Pd-AS, Zn-AS and the corresponding pure-titania system (TiO_2-AS). The vertical arrows indicate the intermediate temperatures selected for reductive treatment of Pd-AS system.

the decomposition of palladium oxide into Pd and oxygen which has been reported to occur on calcination at high temperatures [13,19].

In order to gain more information on the surface composition of the systems, XPS analyses were carried out. The main features concerning XPS characterization of our samples are summarized in Table 2.

The determination of the nature and oxidation state of Pd species (Pd^0, Pd^{2+} and Pd^{4+}) can be carried out through the study of Pd $3d_{5/2}$ XPS peak. It is known that metallic Pd^0 has binding energies of 334.9 ± 0.2 eV [21–23] while palladium in oxidized states, Pd^{2+} and Pd^{4+} exhibits much higher binding energies: 336.4 eV ($3d_{5/2}$) for Pd^{2+} [24] and 337.6 eV ($3d_{5/2}$) for Pd^{4+} [20] in PdO and PdO_2, respectively [25].

Pd 3d signals obtained for all our Pd-containing systems are depicted in Fig. 4A. In the region of palladium, the original sample (Pd-AS), showed a XPS profile which is relatively complex in which one can identify broad peaks centered around 336.4 eV and 341.7 eV corresponding to $3d_{5/2}$ and 3 $d_{3/2}$ peaks respectively. On closer inspection, the broad peak at 336.4 eV, might be considered as the result of two components, a peak located at 336.4 eV attributed to Pd^{2+} $3d_{5/2}$ together with a shoulder peak at 337.6 eV assigned to Pd^{4+} $3d_{5/2}$. Thus, it can be inferred that in the original sample, the valence states of Pd are Pd^{2+}/Pd^{4+}.

The oxidation treatment of the original sample, either in air flux or calcination in air at 850 °C, led to a Pd-XPS profile in which palladium $3d_{5/2}$ peaks around 336.4 eV are identified indicating the presence of Pd^{2+} (probably as PdO) at the catalyst surface. The fact that Pd^0 is not detected by XPS but observed through XRD, suggests that such species are present in the bulk of Pd-850-AIR. After reduction in H_2/Ar flux at 200 °C (Pd-200-H), only a palladium $3d_{5/2}$ peak at 334.9 eV is observed thus indicating the presence of Pd^0 and no further change in Pd_{3d} spectrum is observed on reduction at 500 °C (Pd-500-H). Therefore, peaks observed in TPR profile centered at 273 and 400 °C could be assigned to reduction of bulk palladium oxide. In the case of Pd-850-H the band is slightly shifted to lower binding energy (334.6 eV) which could be ascribed to a greater metal–support interaction [9].

XPS data concerning TiO_2 matrix for Pd/TiO_2 samples are depicted in Table 2. Ti^{3+} line position is expected at about 457.5 eV while that of Ti^{4+} (the dominant peak) is located at 458.5 eV [25]. Therefore, binding energies for Ti $2p_{3/2}$ peaks of our samples at 458.4 ± 0.1 eV clearly correspond to Ti^{4+} in TiO_2 structure. The analyses of the Ti 2p spectra did not allow detecting any considerable amount of Ti^{3+} ions. However, by examining the chemical composition on the surface from XPS, it is worth mentioning that the O/Ti ratios for some samples (especially Pd-AS and Pd-850-F) are slightly below the stoichiometric value (O/Ti ~ 2.0). From these results it is expected for those samples the presence of a certain number of oxygen vacancies. In agreement with the previous comments on $Pd_{5/2}$ XP spectrum of Pd-850-H sample, there is a slight shift in Ti $2p_{3/2}$ binding energy to higher values which again suggest a strong Pd–Ti interaction.

Regarding O (1s) band it is noteworthy that for all the samples except for Pd-500-H, a main peak is detected at a

Table 2
Summary of XPS data concerning Pd- and Zn-containing titania used in the present study

Photocatalyst	Ti ($2p_{3/2}$) binding energy (eV)	O (1s) binding energy (eV)	Pd ($3d_{5/2}$) binding energy (eV)	Zn ($2p_{3/2}$) binding energy (eV)	C atomic%	O/Ti	Metal/Ti atomic%
Pd-850-F	458.4	529.6	336.3	Not applicable	4.1	1.86	0.5
Pd-850-AIR	458.3	529.7	336.0		5.2	1.90	0.8
Pd-AS	458.3	529.6	336.4		5.1	1.75	0.9
Pd-200-H	458.3	529.6	334.9		9.1	1.99	0.9
Pd-500-H	459.1	530.6	334.8		7.7	1.95	0.8
Pd-850-H	458.5	529.9	334.6		4.5	2.09	3.1
Zn-850-AIR	458.1	526.0; 529.4; 531.7	Not applicable	1021.4	0.3	2.17	14.3
Zn-AS	458.4	. . .; 529.7; 531.7		1024.5	5.3	2.02	3.3
Zn-850-H	458.6	. . .; 529.3; 531.7		–[a]	6.4	2.16	–[a]

[a] Quantification of zinc atomic% present at the surface of Zn-850-H was not possible since the intensity of Zn(2p) peak was very small.

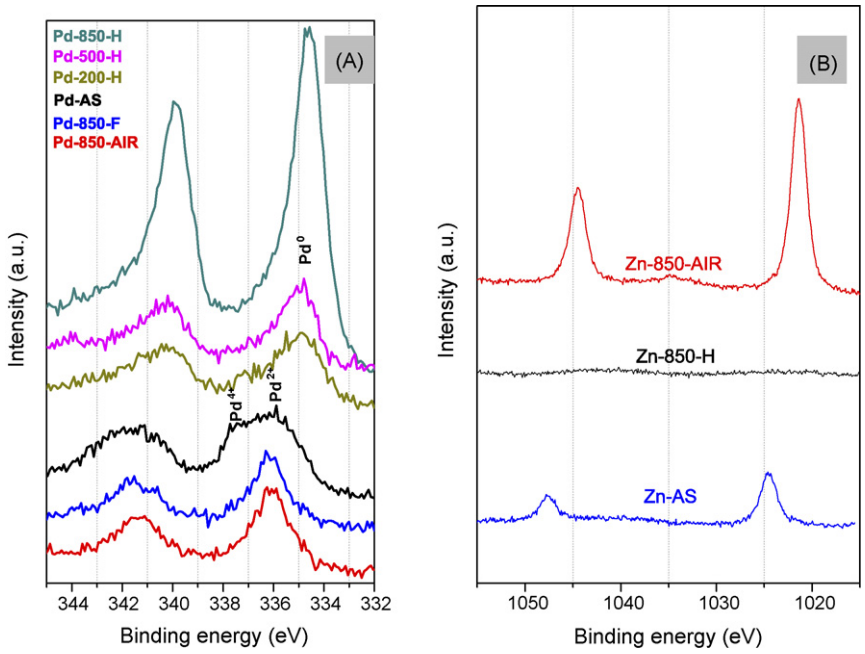

Fig. 4. Pd 3d (A) and Zn 2p (B) XP spectra of different systems.

binding energy of 529.7 ± 0.2 eV which is ascribed to lattice oxygen in TiO_2.

The case of Pd-500-H is particularly interesting since it presented a shift of both Ti2p and O1s signals to higher binding energies. Such a change must reflect a change in Ti–O charge distribution and cannot be assigned to different experimental conditions, since all Pd-samples were recorded on the charge compensation mode. Moreover, position of adventitious carbon and palladium signals do not change for that sample as compared, for instance, to Pd-200-H sample. Ti2p binding energy at 459.1 can be ascribed to Ti (4+) [26] in Ti–O bonds though with lower covalence than in the other samples [27,28]. As for the increase in binding energy of O1s it could be explained in terms of formation of surfacial OH species as the result of hydrogen treatment at 500 °C. Any treatment of the samples at 850 °C results in partial/complete transformation of anatase into rutile and Ti–O charge distribution is again more similar to the samples calcined at $T \leq 500$ °C.

As far as atomic Pd/Ti ratios are concerned, such values are between 0.5% and 0.9% for all samples but for Pd-850-H (3.1%). In that latter case, reductive treatment at 850 °C is accompanied by a significant surfacial increase in palladium content (5-fold as compared to the bulk one, as determined by ICP-MS). TEM micrographs of such sample (depicted in Fig. 5) show the presence of palladium particles with a size of 5–20 nm.

Photocatalytic behaviour of all palladium-samples for gas-phase selective photoxidation of 2-propanol are shown in Fig. 2. For comparative purposes, results obtained with the corresponding bare-titania systems synthesized under identical conditions as palladium-containing ones have been included. Finally, Degussa P25, a well-known reference titania system was also tested.

As can be observed, reduction of Pd-AS at temperatures up to 500 °C leads to a gradual increase in catalytic activity; so much so that Pd-500-H system exhibits even higher initial activity than Degussa P25. The increase in catalytic performance on reduction temperature could be ascribed to the transformation of $Pd^{\delta+}$ to Pd^0, the latter species being more active. This would suggest that TPR peaks observed at $T \leq 400$ °C are due to reduction of bulk palladium oxide, since XPS results showed that palladium on the surface had already been reduced at 200 °C. Thermal treatments at 850 °C resulted in a decrease in photocatalytic activity. This is hardly surprising since at those high temperatures the systems exhibit very low surface areas. Catalytic activity of Pd-850-AIR is significantly higher than that of Pd-850-F which again could be ascribed to the presence of Pd^0 in the former system, as a result of decomposition of palladium oxide (as evidenced by XRD). Moreover, both systems are more active than the bare-titania system TiO_2-850-AIR.

On the contrary, catalytic activity of Pd-850-H and TiO_2-850-H is quite similar. In this case, there could be two different effects. On one hand, the presence of Pd^0 would tend to favour the reaction; on the other, palladium surface content could result too high, palladium particles thus acting as recombination centers. Pichat et al. found that there is an optimal metal/titania ratio below which the metal reduces the charge recombination in TiO_2 whereas above such a value recombination at the metal particles progressively cancels such a beneficial effect [29].

As far as selectivity is concerned, calcination of all systems at 850 °C results in an increase in selectivity to acetone. At first sight, this could seem to suggest that either rutile particles are more selective to acetone than anatase ones or that the lower the surface area, the higher the selectivity to acetone. However, the fact that TiO_2-AS (100% anatase, 121 m^2/g) and Degussa-P25 (20% rutile/80% anatase, 50 m^2/g) exhibited similar selectivities to acetone appears to rule out such hypotheses. It could be

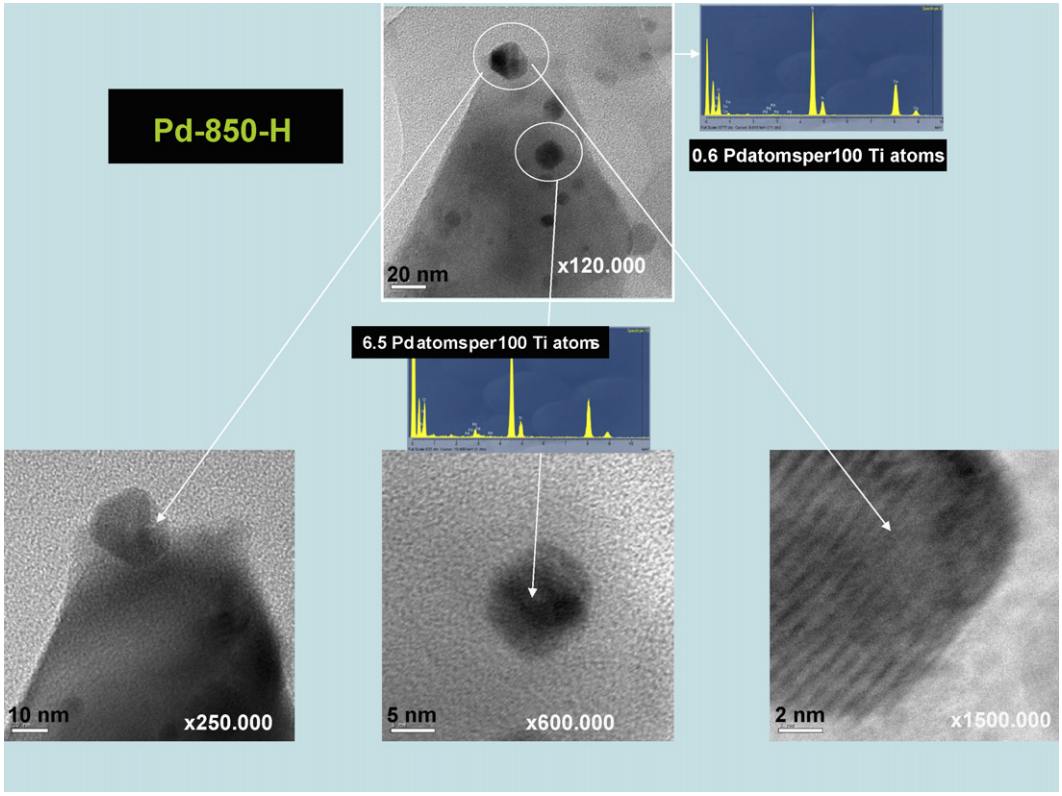

Fig. 5. TEM micrographs and EDX analyses of Pd-850-H.

also possible that the higher selectivity to partial oxidation product (acetone) on calcination at high temperatures be somehow associated to the lower availability of surface hydroxyl species and lattice oxygen [30]. Nevertheless, this requires further studies.

In the case of Pd-850-H even though it shows similar conversion values as TiO_2-850-H (18–20% after 5 h), selectivity to acetone is much higher (97 and 87% for Pd-850-H and TiO2-850-H, respectively), thus indicating that the increase in the surface palladium content is accompanied by an increase in selectivity to acetone.

In order to rule out the possibility of thermal activity, an experiment on Pd-500-H (the most-active palladium system) was carried out (Fig. 6). After 80 min of photocatalytic reaction, a shutter is closed thus preventing the light to reach the catalyst. Under such circumstances, molar conversion drops from 42.9% (point one) to 6.4 and 2.3% (points 2 and 3). The shutter is then opened and conversion is recovered (points 4 and 5). Light output was then adjusted to 83% the initial value, thus resulting in a ca. 16% decrease in 2-propanol conversion (points 6 and 7). If light output is again adjusted to 100% intensity, conversion increases again (point 8). Finally, we used a heat ray

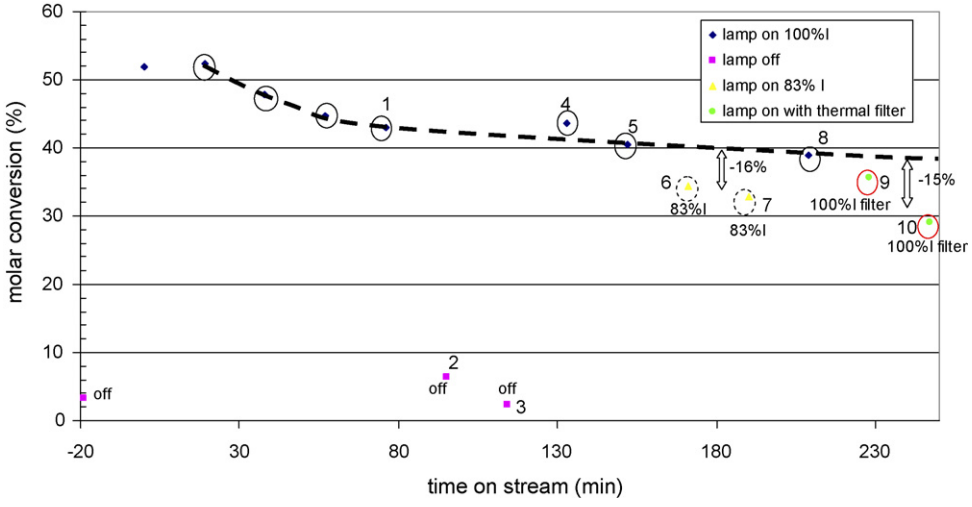

Fig. 6. Different tests carried out to evidence the negligible thermal effect in gas-phase selective photooxidation of 2-propanol on Pd-500-H.

cutting filter (Hamamatsu Ref. A7028-03, cut wavelength 400–700 nm). Under such conditions, UV transmittance dropped from 1.1 to 0.9 W/cm^2 (17% decrease) which had the same effect on molar conversion (points 9 and 10) as to adjust light output to 83% intensity (points 6 and 7). Therefore, we can conclude that no significant thermal effect is observed under our experimental conditions and, consequently, photocatalytic activity is to account for 2-propanol transformation.

3.2. Case study #2: Zn-containing systems

Data concerning characterization of Zn-containing samples are collected in Table 1. As can be seen, the starting material Zn-AS is formed by 100% anatase particles, with a crystallite size of 19 nm and a surface area of 59 m^2/g. Experimental Zn/Ti ratio (as determined by ICP-MS) is slightly below the nominal one (0.7 and 1%, respectively). Moreover, XPS results seem to suggest that Zn is preferentially located at the surface, since this technique gives a Zn/Ti ratio of 3.3%.

Results found for catalytic activity of Zn-AS in gas-phase 2-propanol selective photooxidation are represented in Fig. 7. From that figure it is clear that Zn-AS exhibits higher initial activity than the corresponding bare-titania system (TiO_2-AS). Nevertheless, situation after 5 h is the opposite due to the higher deactivation of Zn-AS as compared to TiO_2-AS. As far as selectivity to acetone is concerned both systems show similar values (ca. 75% for $t = 5$ h).

In a similar way as described for Pd-AS, a TPR profile was collected for Zn-AS (Fig. 3). In this case, there is only one peak centered at ca. 528 °C, which is in agreement with that reported in the literature [31].

In order to study the effect of oxidative and reductive calcination treatments on the photocatalytic activity of Zn-AS, the system was submitted to calcination at 850 °C in static air (Zn-850-F), air (Zn-850-AIR) or hydrogen (Zn-850-H) flow. Some data regarding characterization of such systems are collected in Table 1. Therefore, in all cases, calcination at 850 °C leads to the transformation of anatase into rutile which is accompanied by a significant increase in crystallite size and a dramatic decrease in surface area. XRD patterns plotted in Fig. 1B do not show any zinc crystal phase which could be due to the low content in Zn or the low crystallite size. In order to cast further light on the location of zinc in the solids they were studied by XPS.

XPS studies showed that there were four kinds of elements, carbon, zinc, titanium and oxygen, on the surface of the Zn/TiO_2 samples. For all the studied samples, the binding energy for Ti $2p_{3/2}$ was found at around 458.3 ± 0.3 eV which is consistent with that reported for titanium in TiO_2.

The XPS spectra of the Zn_{2p} for Zn-AS, Zn-850-H and Zn-850-AIR are depicted in Fig. 4B. Therefore, in the original catalysts calcined at 500 °C (Zn-AS) there are two peaks at 1047.7 and 1024.5 eV which correspond to the binding energies of Zn $2p_{1/2}$ and Zn $2p_{3/2}$, respectively. According to the handbook of the XPS instrument and the literature data for ZnO samples [25,32], the binding energies of Zn $2p_{1/2}$ and Zn $2p_{3/2}$ are observed at 1044.5 and 1021.4 eV, respectively which are typical of Zn^{2+} forming bonds with oxygen atoms. However, the shift of ca. 3.1 eV to higher binding energies which are observed for the Zn 2p peaks in the original Zn/TiO_2 sample could be explained by assuming the possibility of Zn^{2+} substituting the lattice position of Ti^{4+} in TiO_2 crystalline. Based on the surface Zn/Ti atomic ratio (Table 2) it can be inferred that in Zn-AS, the Zn^{2+} ions are mainly located at the surface rather than in the bulk.

As far as O 1s peak for Zn-AS is concerned (not presented), it was asymmetric (the left side is wider than that of the right) indicating that at least two kinds of oxygen species were

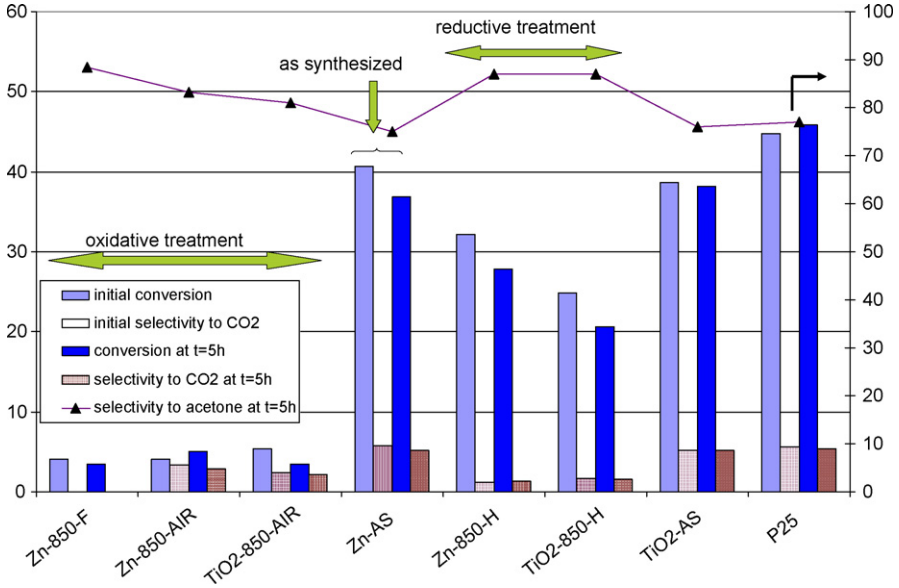

Fig. 7. Results obtained for gas-phase selective photooxidation of 2-propanol with all the Zn-containing titania described in the present study in terms of molar conversion (%), selectivity to acetone (%) and selectivity to CO_2 (%). For the sake of comparison, results obtained with the corresponding bare-titania systems as well as Degussa P25 have also been included.

present in the near surface region. The main intense peak at about 529.7 eV could be ascribed to crystal lattice oxygen, while the peak at about 531.7 eV could be associated to oxygen probably as carbonate species; in fact a certain amount of carbonaceous species were detected in this sample, probably arisen from carbonate species after calcination of the organic precursor.

The oxidation treatment of the original sample, in air flux at 850 °C (Zn-850-AIR), led to a Zn-XPS profile in which peaks around 1021.4 eV and 1044.5 eV are identified, which are typical of Zn^{2+} binding to oxygen atoms. Regarding the O 1s peak from that sample, at least three peaks are observed. They are centered at 526.0, 529.4 and 531.7 eV, respectively, the peak at 529.4 eV being the most intense. The high binding-energy component is usually attributed to the presence of loosely bound oxygen on the ZnO nanocrystals [33–35]. The main intense peak at 529.4 eV could be ascribed to crystal lattice oxygen of TiO_2. However, a certain amount of this intense peak could be attributed to O^{2-} ions on wurtzite structure of hexagonal Zn^{2+} ion array, surrounded by Zn atoms with their full complement of nearest-neighbour O^{2-} ions [36,37]. Although in the absence of a very accurate fitting of the O 1s peak, we cannot estimate the amount of this component, it is noteworthy that the intensity of this component measures the amount of oxygen atoms in a fully oxidized stoichiometric surrounding [38].

From the statistical results of XPS, we could infer that the atomic Zn/Ti ratio was 3.3% for the original sample Zn-AS and 14.3% for Zn-850-AIR (Table 2). Moreover, the O/Ti ratio was found above the stoichiometric value. Therefore, some zinc atoms which occupied lattice positions in titania structure in Zn-AS system segregated and migrated to the surface where they formed small ZnO clusters not observable by XRD. Actually, EDX studies on Zn-850-AIR sample (not presented) showed very different Ti/Zn composition depending on the area analyzed which supports the idea of the existence of such clusters.

The XPS study of Zn-850-H showed a surface in which Zn^{2+} was practically absent (very low indeed). Moreover, ICP-MS analyses (Table 1) showed that such sample had overcome a significant decrease in the Zn content (atomic metal/Ti% was 0.7 and 0.3 for Zn-AS and Zn-850-H, respectively). This suggests the sublimation of Zn which has been reported to occur at appreciable rate at ca. 600 °C [39].

As far as the photocatalytic behaviour is concerned, results found for 2-propanol photoselective oxidation are shown in Fig. 7. As can be observed, neither the oxidative nor the reductive treatment of Zn-AS at 850 °C resulted in any increase in 2-propanol molar conversion. It seems that the formation of ZnO agglomerates on the surface of Zn-850-AIR is particularly detrimental to activity whereas Zn-850-H in which there is no zinc on the surface but in the bulk is more active than the corresponding pure titania-TiO_2-850-H (molar conversion being 27.8 and 20.7 after 5 h on stream, respectively). Finally, as already described for Pd-systems, thermal treatment led to an increase in selectivity to acetone.

4. Conclusions

The above-mentioned results allow us to draw the following conclusions:

Oxidation/reduction calcination treatments of two Pd- or Zn-containing titania systems led to significant changes structural and textural changes which, in turn, resulted in differences in photocatalytic performance as measured for gas-phase selective photooxidation of 2-propanol.

As regards the Pd-systems, reduction of the original sample (Pd-AS) at $T \leq 500$ °C resulted in a gradual increase in its catalytic activity, which is ascribed to the reduction of bulk palladium. Thermal treatment at 850 °C led to a significant decrease in catalytic performance which can be explained in terms of the sharp drop in surface area of the materials. Nevertheless, systems calcined at 850 °C containing Pd^0 are more active than the one consisting of PdO particles only. Moreover, palladium migrated to the catalyst surface on reduction at 850 °C which resulted in an increase in selectivity to acetone (ca. 97%).

As far as Zn-systems are concerned, the most favourable situation for activity seems to be that in which Zn atoms substitute Ti ones in the lattice whereas the observed segregation of Zn atoms and migration to the surface to form ZnO clusters is especially detrimental to activity.

In all the cases, systems calcined at 850 °C were more selective to acetone than those treated at $T \leq 500$ °C, which could be ascribed to the less availability of hydroxyl groups or lattice oxygen in those systems, thus limiting complete oxidation of 2-propanol.

Acknowledgements

The authors wish to acknowledge financial support from the Consejería de Educación y Ciencia of the Junta de Andalucía (Project FQM 191) and the Spanish Ministerio de Educación y Ciencia (Projects CTQ 2005-04080/BQU, CTQ2007-65754 and CTQ 2004-05734-C02-02, co-financed with FEDER funds). Finally, Dr. Colmenares is thankful to the Spanish Ministerio de Educación, Cultura y Deportes for a post-doctoral fellowship and A. Marinas to Junta de Andalucía for a contract.

References

[1] X. Zhang, F. Zhang, K.-Y. Chan, Mater. Chem. Phys. 97 (2006) 384.
[2] P. Pichat, New. J. Chem. 11 (1987) 135.
[3] M. Álvaro, C. Aprile, M. Benítez, E. Carbonell, H. García, J. Phys. Chem. B 110 (2006) 6661.
[4] S.-Y. Kim, T.-H. Lim, T.-S. Chang, C.-H. Shin, Catal. Lett. 117 (2007) 112.
[5] P. Evans, S. Mantke, A. Mills, A. Robinson, D.W. Sheel, J. Photochem. Photobiol. A 188 (2007) 387.
[6] J.C. Colmenares, M.A. Aramendia, A. Marinas, J.M. Marinas, F.J. Urbano, Appl. Catal. A 306 (2006) 120.
[7] S.A. Larson, J.A. Widegren, J.L. Falconer, J. Catal. 157 (1995) 611.
[8] U.R. Pillai, E. Sahle-Demessie, J. Catal. 211 (2002) 434.
[9] M.A. Aramendía, J.C. Colmenares, A. Marinas, J.M. Marinas, J.M. Moreno, J.A. Navío, F.J. Urbano, Catal. Today 128 (2007) 235.
[10] S.J. Tauster, S.C. Fung, R.L. Garten, J. Am. Chem. Soc. 100 (1978) 170.

[11] M. Bowker, P. Stone, R. Bennett, N. Perkins, Surf. Sci. 497 (2002) 155.
[12] M. Zhang, Z. Jin, Z. Zhang, H. Dang, Appl. Surf. Sci. 250 (2005) 29.
[13] C.-B. Wang, H.-G. Lee, T.-F. Yeh, S.-N. Hsu, K.-S. Chu, Thermochim. Acta 401 (2003) 209.
[14] U.-S. Ozkan, M.W. Kumthekar, G. Karakas, Catal. Today 40 (1998) 3.
[15] V. Ferrer, A. Moronta, J. Sánchez a, R. Solano, S. Bernal, D. Finol, Catal. Today 107–108 (2005) 487.
[16] K.-I. Shimizu, S. Koizumi, T. Hatamachi, H. Yoshida, S. Komai, T. Kodama, Y. Kitayama, J. Catal. 228 (2004) 141.
[17] N. Macleod, J.M. Keel, R.M. Lambert, Appl. Catal. A 261 (2004) 37.
[18] V. Narayana Kalevaru, A. Benhmid, J. Radnik, M.-M. Pohl, U. Bentrup, A. Martin, J. Catal. 246 (2007) 399.
[19] W. Lin, L. Lin, Y.X. Zhu, Y.C. Xie, K. Scheurell, E. Kemnitz, J. Mol. Catal. A 226 (2005) 263.
[20] Y. Bi, G. Lu, Appl. Catal. B 41 (2003) 279.
[21] V.V. Kaichev, M. Morkel, H. Unterhalt, I.P. Prosvirin, V.I. Bukhtiyarov, G. Rupprechter, H.-J. Freund, Surf. Sci. 566–568 Pt. (2) (2004) 1024.
[22] A.-S. Mamede, G. Leclercq, E. Payen, P. Granger, L. Gengembre, J. Grimblot, Surf. Interf. Anal. 34 (2002) 105.
[23] O. Demoulin, M. Navez, P. Ruiz, Catal. Lett. 103 (2005) 149.
[24] G. Ketteler, D.F. Ogletree, H. Bluhm, H. Liu, E.L.D. Hebenstreit, M. Salmeron, J. Am. Chem. Soc. 127 (2005) 18269.
[25] J.F. Moulder, W.F. Stickle, P.E. Sobol, K. Bomben, in: J. Chastain (Ed.), second ed., Handbook of X-Ray Photoelectronic Spectroscopy, Perkin-Elmer Corporation (Physical Electronics), 1992.
[26] Y.Z. Yang, C.-H. Chang, H. Idriss, Appl. Catal. B 67 (2006) 217.
[27] T.L. Barr, M.A. Lishka, J. Am. Chem. Soc. 108 (1986) 3178.
[28] T.L. Barr, Zeolites 10 (1990) 760.
[29] P. Pichat, J.M. Herrmann, J. Disdier, M.N. Mozzanega, H. Courbon, Stud. Surf. Sci. Catal. 19 (1984) 319.
[30] C. Doornkamp, V. Ponec, J. Mol. Catal. A 162 (2000) 19.
[31] J. Silvestre-Albero, J.C. Serrano-Ruiz, A. Sepúlveda-Escribano, F. Rodríguez-Reinoso, Appl. Catal. A 292 (2005) 244.
[32] L. Jing, Z. Xu, J. Shang, X. Sun, W. Cai, H. Guo, Mater. Sci. Eng. A332 (2002) 356.
[33] M. Koudelka, A. Monnier, J. Sánchez, J. Mol. Catal. 25 (1984) 295.
[34] R. Cebulla, R. Weridt, K. Ellmer, J. Appl. Phys. 83 (1998) 1087.
[35] Y. Du, M.-S. Zhang, Y. Shen, Q. Chen, Z. Yin, Appl. Phys. A76 (2003) 171.
[36] L.K. Rao, V. Vinni, Appl. Phys. Lett 63 (1993) 608.
[37] J.C.C. Fan, J. Appl. Phys. 48 (1977) 3524.
[38] M. Chen, X. Wang, Y.H. yu, Z.L. Pei, et al. Appl. Surf. Sci. 158 (2000) 301.
[39] O.W. Perez-Lopez, A.C. Farias, N.R. Marcilio, J.M.C. Bueno, Mater. Res. Bull. 40 (2005) 2089.